

See discussions, stats, and author profiles for this publication at: <https://www.researchgate.net/publication/265135703>

Functional Water Molecules in Rhodopsin Activation

ARTICLE *in* THE JOURNAL OF PHYSICAL CHEMISTRY B · AUGUST 2014

Impact Factor: 3.3 · DOI: 10.1021/jp505180t · Source: PubMed

CITATIONS

2

READS

61

3 AUTHORS:



Xianqiang Sun

Washington University in St. Louis

22 PUBLICATIONS 95 CITATIONS

[SEE PROFILE](#)



Hans Agren

KTH Royal Institute of Technology

867 PUBLICATIONS 18,824 CITATIONS

[SEE PROFILE](#)



Yaoquan Tu

KTH Royal Institute of Technology

70 PUBLICATIONS 633 CITATIONS

[SEE PROFILE](#)

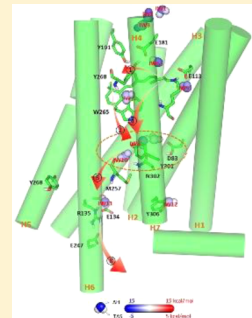
Functional Water Molecules in Rhodopsin Activation

Xianqiang Sun, Hans Ågren, and Yaoquan Tu*

Division of Theoretical Chemistry and Biology, School of Biotechnology, KTH Royal Institute of Technology, S-106 91 Stockholm, Sweden

S Supporting Information

ABSTRACT: G-protein-coupled receptors (GPCRs) are integral membrane proteins that mediate cellular response to an extensive variety of extracellular stimuli. Studies of rhodopsin, a prototype GPCR, have suggested that water plays an important role in mediating the activation of family A GPCRs. However, our understanding of the function of water molecules in the GPCR activation is still rather limited because resolving the functional water molecules solely based on the results from existing experiments is challenging. Using all-atom molecular dynamics simulations in combination with inhomogeneous fluid theory, we identify in this work the positioning of functional water molecules in the inactive state, the Meta II state, and the constitutive active state of rhodopsin, basing on the thermodynamic signatures of the water molecules. We find that one hydration site likely functions as a switch to regulate the distance between Glu181 and the Schiff base in the rhodopsin activation. We observe that water molecules adjacent to the “Np_xxY” motif are not as stable in the Meta II state as in the inactive state as indicated by the thermodynamics signatures, and we rationalize that the behaviors of these water molecules are closely correlated with the rearrangement of the water-mediated hydrogen-bond network in the “NP_xxY” motif, which is essential for mediating the activation of the receptor. We thereby propose a hypothesis of the water-mediated rhodopsin activation pathway.



INTRODUCTION

G-protein-coupled receptors (GPCRs) comprise the largest family of membrane proteins that sense a wide range of extracellular stimuli to regulate cytoplasmic signal transduction pathways. Upon agonist binding, activation of a GPCR is initiated, which further activates intracellular signal transduction pathways.^{1–7} Inspection of GPCR crystal structures has suggested that the activation of GPCRs is mediated by structural water molecules, given that conserved water molecules are found to be colocalized in the helical bundle of most of the resolved GPCR structures.^{8–12} This notion has been supported by the radiolytic footprinting analysis, which has revealed that conformational changes in rhodopsin, a prototype GPCR, are likely mediated by the dynamics of water molecules and their interaction with the protein side chains.⁸ A recent structural analysis of a constitutively active rhodopsin has further indicated that GPCR activation is accompanied by a reorganization of water-mediated hydrogen-bond networks between some of the most conserved residues in the GPCR.¹³ Despite such advances, our understanding of the functions of water molecules in GPCR activation is still very limited, mainly because it is still difficult to recover all the functional water molecules from crystal structures where water molecules can be partially occupied¹⁴ or with other experimental approaches.

Our strategy is to apply molecular dynamics (MD) simulations in combination with inhomogeneous fluid theory (IFT)^{15–18} to locate the water molecules and to identify the functional water molecules in rhodopsin. IFT determines the thermodynamic signature of a hydration site solely based on the distribution of water molecules around the site,¹⁵ which allows

one to determine the positioning of the functional water molecules in rhodopsin in a membrane environment. IFT analysis can be applied to study the interfacial water molecules or water molecules in the vicinity of a solute.¹⁹ It has been successfully applied to the study of conserved water molecules in ligand binding sites or protein–protein interfaces.^{16,17,20–23}

Water molecules have been suggested to play an essential role in rhodopsin, such as in proton transfer²⁴ and signal transmission.²⁵ In this work, we selected some key states of rhodopsin and applied MD simulations and IFT to each of the selected states to position the functional water molecules and calculate their thermodynamic signatures. Rhodopsin consists of a ligand-free protein moiety of seven transmembrane helices (H1–H7) linked by loops (ECL1–ECL3, ICL1–ICL3), named opsins, and a covalently bound ligand 11-cis retinal. The N terminus of rhodopsin is composed of two short strands and adopts a typical antiparallel β -sheet fold, with ECL2 composed of two β -strands located roughly below it when viewed from the extracellular side. There exist two conserved structural motives of rhodopsin, the “NP_xxY” motif and the “ERY” motif, which have proven to play a pivotal role in the rhodopsin activation. The “NP_xxY” motif with the sequence from Asn302 to Tyr306 on H7 is one of the most conserved motives and rearranges upon receptor activation. The “ERY” motif, which corresponds to the residues from Glu134 to Tyr136 on H3, is another well-characterized rhodopsin motif. There exists an ionic lock between Arg135 on the “ERY” motif and Glu247 on H6. Upon

Received: May 27, 2014

Revised: July 30, 2014

receptor activation, this ionic lock must be broken.²⁶ In the dark, the 11-cis retinal works as an inverse agonist, which constrains the opsin in the inactive conformation. Photoabsorption of the 11-cis retinal leads to the isomerization of the retinal to the all-trans form. During this stage, water molecules work as a temporary energy storage vehicle and reduce the pK_a of the central proton binding site.^{24,27} The latter results in the proton transfer from the protonated Schiff base to Asp85 in bacteriorhodopsin (the corresponding residue in rhodopsin is Glu113) and induces the formation of the all-trans retinal. Comparing of the all-trans retinal with the 11-cis retinal in the ground-state rhodopsin, the β -ionone ring of the all-trans retinal has been found to be 4.3 Å from the cleft between H5 and H6, which makes the all-trans retinal act as a strong agonist for triggering of the activation of rhodopsin.^{13,26,28} The rhodopsin activation undergoes several intermediate states, of which the Meta II state serves as a key state whose structure (PDB ID: 3PXO) has recently been obtained. This structure confirms the outward tilt motion of the H6, which is facilitated by the rearrangement of the water clusters adjacent to the "NPxxY" motif.²⁹ This structure, together with the inactive-state structure (PDB ID: 1U19)³⁰ and the constitutively active-state structure (PDB ID: 2X72), a rhodopsin structure including a constitutively active mutant Glu113Gln,¹³ was chosen for our study of the functional water molecules. We determine the corresponding hydration sites and their thermodynamic signatures in the three structures based on the results of MD simulations and the IFT analysis. By analyzing the distribution of the hydration sites and the evolution of the associated hydrogen-bond networks in different states, we studied the function of water molecules in rhodopsin activation. A rearrangement of the water-mediated hydrogen-bond network in the "NPxxY" motif has been suggested to be essential for mediating the activation of the receptor.¹² We not only reproduced the crystallized water molecules in the "NPxxY" motif for the inactive state, but also identified functional water molecules in this motif in the Meta II and the active states, which have not been reported previously. We found that the rearrangement in the "NPxxY" motif originates from the water-mediated hydrogen-bond network in the Meta II state, which is less stable than in the inactive state as indicated by the thermodynamic signatures of the functional water molecules. We also found that one water molecule between Glu181 and the Schiff base functions as a switch for signaling by regulating the distance between Glu181 and the Schiff base, which hitherto has not been reported.

METHODS

Protein Structure Preparation. The protein structures were retrieved from the Protein Data Bank (PDB).³¹ For the inactive-state structure, the PDB entry 1U19 was selected because this structure is of high resolution.³⁰ For the Meta II state structure, the coordinates were obtained from the PDB entry 3PXO.²⁹ Molecules other than the retinal or protein were removed from these structures. Mutated residues in the constitutively active structure were changed back to the wild type. The disulfide bond between Cys110 and Cys187 was reserved. According to the Fourier-transform infrared spectroscopy study,^{32,33} Asp83 and Glu122 were set to be protonated, whereas Glu113 was set to be protonated in the Meta II and activated states. The protonation state of Glu181 is still controversial because Fourier transform infrared spectroscopy measurements indicated this residue to be charged,³³ while pre-

resonance Raman and UV-vis spectra were in favor of the uncharged state.^{34,35} Jan et al. have revisited the published results on the protonation state of Glu181 and provided strong support for the unprotonated state of Glu181.³⁶ We thus set Glu181 as unprotonated in all the simulations. All the other residues that may have different protonation states were set to the proper protonation states according to the pK_a value for each residue obtained from the protein preparation results at the physiological pH with the Schrödinger software.³⁷ The Schiff base on the retinal was set to be neutral and protonated for the inactive and Meta II states, respectively.³³ In order to effectively retrieve the functional water molecules, we prepared the initial water molecules in each state by merging the cocrystallized water molecules in the three crystal structures, with the overlapping water molecules with the oxygen–oxygen distance less than 1.5 Å simply represented by a single water molecule. The water molecules thus prepared were included in the molecular dynamics simulations.

System Setup. The systems with rhodopsin embedded in the membrane were built using VMD.³⁸ Each protein structure, together with the initial water molecules prepared in the above section, was solvated with TIP3P water molecules in a cubic box, with each side ~12 Å larger than the protein. The protein structure was then aligned with the 1-palmitoyl-2-oleoyl-sn-glycero-3-phosphocholine (POPC) bilayer so that the protein was located in the center of the bilayer, followed by deleting (i) the lipid molecules within 0.8 Å of the protein and (ii) water molecules within 3.0 Å of the protein and remaining lipid molecules. Each system was further neutralized by adding chloride ions. The resulting system for the inactive state rhodopsin consisted of 81 lipid molecules, 3 chloride ions, and 7433 water molecules, with 38671 atoms in total, and measured as $78 \times 65 \times 101$ Å³; the resulting system for the Meta II state rhodopsin consisted of 81 lipid molecules, 6 chloride ions, and 8359 water molecules, with 41154 atoms in total, and measured $78 \times 65 \times 101$ Å³; the resulting system for the active state rhodopsin consisted of 79 lipid molecules, 7 chloride ions, and 8268 water molecules, with 40798 atoms in total, and measured $80 \times 67 \times 103$ Å³.

Molecular Dynamics Simulations. All the MD simulations were carried out with the NAMD 2.8 program³⁹ with CHARMM27 parameter set used for the protein, lipids, and salt ions, and TIP3P model for water. Force field parameters for the ligand molecules were generated with the CHARMM General Force Field (version 2b7) interface (version 0.9.6 beta).⁴⁰ Dihedrals with the penalty scores larger than 50 were recalculated according to the CHARMM parametrization philosophy with the quantum chemistry calculations carried out at the HF/6-31G* level with Gaussian 09.⁴¹ The NPT ensemble was used in the MD simulations with the temperature and pressure set to 300 K and 1 bar, using the Langevin thermostat with a damping coefficient of 1.0/ps. The bonds containing hydrogen atoms were constrained with the SHAKE algorithm and a time step of 2 fs was used. Periodic boundary conditions were applied, and the cut-offs for the electrostatic and van der Waals interactions were set to 12 Å, with the long-range electrostatic interaction recovered by the particle mesh Ewald summation. For each system, the tails of the lipid molecules were melted for 0.5 ns with all the other atoms fixed, followed by another 0.5 ns of relaxation with all the atoms on the protein, ligand, and the localized water molecules constrained by a harmonic potential with the force constant of 10 kcal/mol/Å². Thereafter, a simulation of 20 ns was carried

out with the constraint on the localized water molecules and the hydrogen atoms on the protein removed. The snapshots were saved every 2 ps. We used the number densities of water molecules within 16 Å of the retinal to study the evolution of the water density in the interior of rhodopsin. This is because the region within 16 Å of the retinal is located in the interior of the protein and can cover all the key functional motives of rhodopsin. We can see from Figure S1 that the densities increase sharply at the beginning of the simulations and remain stable thereafter. Because the region we take into account is located in the interior of the protein, we believe that the interior of the protein is fully hydrated in 1 ns (Figure S1). The trajectories in the last 12 ns of the simulation were used for analysis. Functional water molecules correspond to the hydration sites located in energetically favorable regions, and their positions can thus be determined through moderately long MD simulations. Referring to the studies carried out in refs 18 and 20, we believe that the simulation time in this work is sufficiently long for determining the hydration sites and their thermodynamics signatures.

Hydration Site Detection. In order to derive the hydration sites, we used a grid analysis algorithm by dividing the simulation box into cubic subvolumes with sides of length 1.6 Å. A subvolume with the water occupancy probability larger than 25% was considered to be possibly occupied by a hydration site whose position was calculated by averaging the coordinates of the water oxygen. Sites with distance less than 2.4 Å were merged into a single site. The positioning of each hydration site was further optimized by averaging the coordinates of the water oxygen within 1.2 Å of the site over the MD trajectories, in line with prior work.¹⁸ This optimization procedure was carried out repeatedly until the difference between the centers from two consecutive optimizations was less than 0.01 Å or the number of iterations reached 100. Hydration sites whose occupancy rates are larger than 0.80 exhibit very low exchange rates (Table S1), reflecting that they are conserved and possibly occupied by functional water molecules. These hydration sites were selected for the calculation of thermodynamic signatures.

Thermodynamic Signature Estimation. According to the IFT, the entropy difference between a water molecule at a hydration site and in bulk consists of the water–protein term (S_{wp}) and the water–water reorganization term (ΔS_{ww}),

$$\Delta S = S_{wp} + \Delta S_{ww} \quad (1)$$

The water–protein term S_{wp} is calculated as,

$$S_{wp} = -\kappa \frac{\rho}{\Omega} \int g_{wp}(\mathbf{r}, \omega) \ln g_{wp}(\mathbf{r}, \omega) d\mathbf{r} d\omega \quad (2)$$

where κ is the Boltzmann constant, ρ represents the density of bulk water, Ω equals $8\pi^2$, $g_{wp}(\mathbf{r}, \omega)$ is the two-body water–protein correlation function, \mathbf{r} represents the position of the water molecule around the hydration site, and ω indicates the Euler angles of the water molecule with respect to the site. By assuming

$$g_{wp}(\mathbf{r}, \omega) = g_{wp}^{trans}(\mathbf{r}) g_{wp}^{orient}(\omega) \quad (3)$$

we can separate S_{wp} into the translational term, S_{wp}^{trans} , and the orientational term, S_{wp}^{orient} :

$$S_{wp} = S_{wp}^{trans} + S_{wp}^{orient} \quad (4)$$

with

$$S_{wp}^{trans} = -\kappa \rho \int g_{wp}^{trans}(\mathbf{r}) \ln g_{wp}^{trans}(\mathbf{r}) d\mathbf{r} \quad (5)$$

$$S_{wp}^{orient} = -\kappa \frac{\rho}{\Omega} \int g_{wp}^{trans}(\mathbf{r}) \int g_{wp}^{orient}(\omega) \ln g_{wp}^{orient}(\omega) d\mathbf{r} d\omega \quad (6)$$

where S_{wp}^{trans} describes the translational ordering of the water molecule around the hydration site, and S_{wp}^{orient} is the orientational distribution of the water molecule at the hydration site.

The water–water reorganization entropy ΔS_{ww} for each hydration site is calculated as the difference between the water–water correlation entropy pertaining to the hydration site and the bulk water

$$\Delta S_{ww} = \sum S_{ww} - S_{bulk} \quad (7)$$

where $\sum S_{ww}$ is the sum of two-body water–water correlation entropies and S_{bulk} represents the entropy of a water molecule in bulk.

Similar to the calculation of water–protein correlation entropy, S_{ww} is also separated into the translational term (S_{ww}^{trans}) and the orientational term (S_{ww}^{orient}),

$$S_{ww} = S_{ww}^{trans} + S_{ww}^{orient} \quad (8)$$

With the Kirkwood superposition approximation (KSA) which assumes that the pair correlation function in an inhomogeneous solvent is equal to that in the bulk solvent and is only dependent on the distance and relative orientation between the two solvent molecules, S_{ww}^{trans} and S_{ww}^{orient} can be approximated as

$$S_{ww}^{trans} = -\frac{1}{2} \kappa \rho^2 \int g_{wp}^{trans}(\mathbf{r}) g_{wp}^{trans}(\mathbf{r}') \{ g_{ww}^{bulk}(R) \ln g_{ww}^{bulk}(R) - g_{ww}^{bulk}(R) + 1 \} d\mathbf{r} d\mathbf{r}' \quad (9)$$

$$S_{ww}^{orient} = -\frac{1}{2} \kappa \rho^2 \int g_{wp}^{trans}(\mathbf{r}) g_{wp}^{trans}(\mathbf{r}') g_{ww}^{bulk}(R) \int g_{ww}^{orient}(\omega) g_{ww}^{orient}(\omega') \{ g_{ww}^{bulk}(\omega|R) \ln g_{ww}^{bulk}(\omega|R) \} d\mathbf{r} d\mathbf{r}' d\omega d\omega' \quad (10)$$

where g_{ww}^{orient} is the water–water orientational correlation function, and g_{ww}^{bulk} is the water–water correlation function in bulk. \mathbf{r}' is the position of the second water molecule with respect to the hydration site, and ω' indicates the Euler angles of the second water molecule with respect to the site. R is the distance between the two hydration sites. $\omega'|R$ is the relative Euler angle of two water molecules at distance R . $g_{ww}^{bulk}(\omega|R)$ is a factorized five-dimensional orientational function in bulk water given as⁴²

$$g_{ww}^{bulk}(\omega|R) = g(\theta_1, \theta_2|R) g(\theta_1, \chi_2|R) g(\theta_2, \chi_1|R) g(\chi_1, \chi_2|R) g(\phi|R)/g(\theta_1|R) g(\theta_2|R) g(\chi_1|R) g(\chi_2|R) \quad (11)$$

The average interaction energy for each hydration site is decomposed into the water–protein term (E_{wp}), water–lipid term (E_{wl}), and water–water term (E_{ww}):

$$E_{int} = E_{wp} + E_{wl} + \frac{1}{2} E_{ww} \quad (12)$$

As the $P\Delta V$ term is negligible, the enthalpy change of the hydration site can be approximated as the difference in the interaction energy of a water molecule at the hydration site and in bulk:

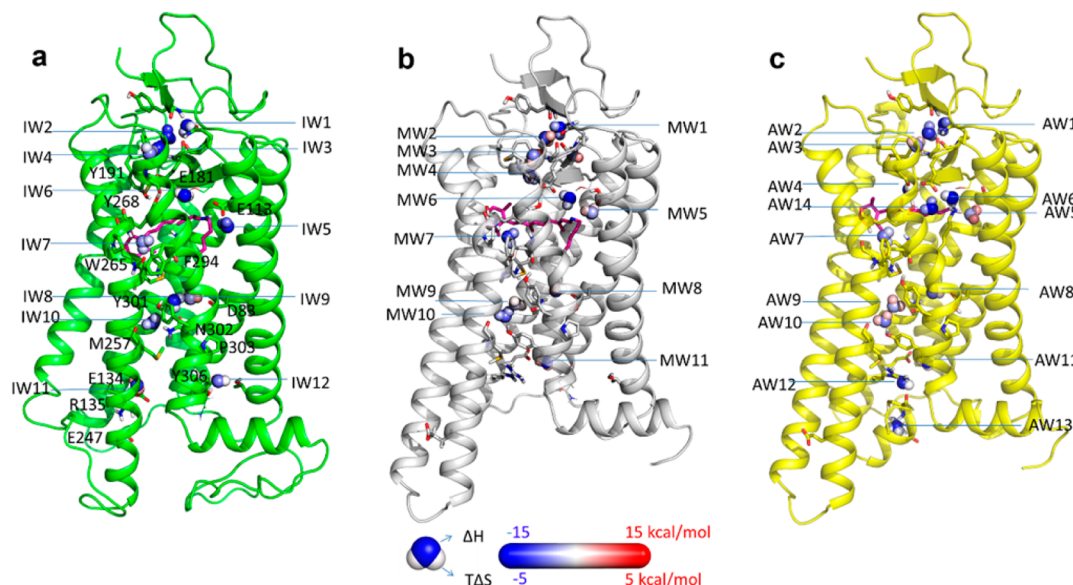


Figure 1. Functional hydration sites with thermodynamic signatures in rhodopsin in the inactive state (a), Meta II state (b), and constitutively active state (c). In each state, the protein is shown as cartoon with the retinal (purple) and key residues shown as sticks. Each hydration site is represented by a corresponding water molecule with atoms shown as spheres. Changes of the thermodynamic signatures, ΔH and $T\Delta S$, of the hydration site are illustrated with the colors on the oxygen and hydrogen atoms of the water molecule according to the spectrum bar shown in the bottom. The same representation method is used in Figures 2, 3, 4, and 5.

$$\begin{aligned} \Delta H &= E_{\text{int}} - \frac{1}{2}E_{\text{bulk}} \\ &= E_{\text{wp}} + E_{\text{wl}} + \frac{1}{2}E_{\text{ww}} - \frac{1}{2}E_{\text{bulk}} \end{aligned} \quad (13)$$

E_{bulk} represents the potential energy required for removing one water molecule from bulk water.

In this work, S_{bulk} was calculated in the same way as the calculation for S_{ww} . This value is -12.6 cal/mol/K obtained from the simulation of a bulk water system of 553 TIP3P water molecules at 300 K for 10 ns. E_{bulk} is -20.40 kcal/mol and was calculated as the total potential energy difference between the two bulk water systems of 553 and 552 TIP3P water molecules obtained from the simulations at 300 K for 10 ns.

Finally, the change of the solvation free energy of a water molecule at the hydration site can be obtained with the following equation:

$$\begin{aligned} \Delta G_{\text{sol}} &= \Delta H - T\Delta S \\ &= E_{\text{wp}} + E_{\text{wl}} + \frac{1}{2}E_{\text{ww}} - \frac{1}{2}E_{\text{bulk}} \\ &\quad - T(S_{\text{wp}} + \Delta S_{\text{ww}}) \end{aligned} \quad (14)$$

RESULTS

Hydration Sites Identified in Rhodopsin. Using the grid analysis algorithm, we identified 41, 23, and 29 hydration sites in the inactive, Meta II, and constitutively active states, respectively (Supporting Information Figure S2). Free energy analysis based on IFT indicated that 38, 21, and 27 hydration sites are located in energetically favorable regions (Figure 1, Data set S1, and Supporting Information). Referring to the cocrystallized water molecules, we found that most of the regions occupied by the cocrystallized water molecules are also covered by the hydration sites, reflecting that our methodology can serve as an important complementary in locating conserved

water molecules in the crystal structures. For the inactive structure 1U19, we found that 17 of the 41 hydration sites are in the regions occupied by the 29 cocrystallized water molecules with the assumption that if the distance between a hydration site and a closest water molecule is less than 2 Å, they are in the same region (Figure S3). We identified 23 hydration sites in Meta II, whereas only 5 water molecules were found to be cocrystallized in it, of which 4 occupy the predicted hydration sites (Figure S4). For the constitutively active state structure 2X72, 11 of the 29 identified hydration sites cover the regions occupied by the cocrystallized water molecules (Figure S5).

Osmolality analysis has indicated a release of about 20 water molecules during the transition from the Meta I to Meta II states.^{26,43} Given that delicate structure rearrangements from the Meta I state to the inactive state have been revealed by the electron crystallography structural analysis⁴⁴ and that the activation transition from the inactive to the Meta I states has been observed even in dried film experiment,⁴⁵ we can assume that water molecules are conserved during the transition from the inactive state to the Meta I state, and approximately 20 water molecules are released from the inactive to the Meta II states. Our result, which shows a reduction of 18 hydration sites from the inactive to the Meta II states, is thus consistent with the osmolality analysis. An analysis of water distributions in the two states indicates that the releasing of water molecules occurs from the regions adjacent to the intracellular and extracellular sides of the receptor (Figure S6). The transition from the Meta I state to the Meta II state involves the deprotonation of the Schiff base. Comparing the hydration sites between the inactive state and the Meta II state, we did not observe obvious water releasing in the region adjunct to the Schiff base (Figure S6), though it is possible that the deprotonation of the Schiff base reduces the thermostability of the hydration sites adjacent to it.

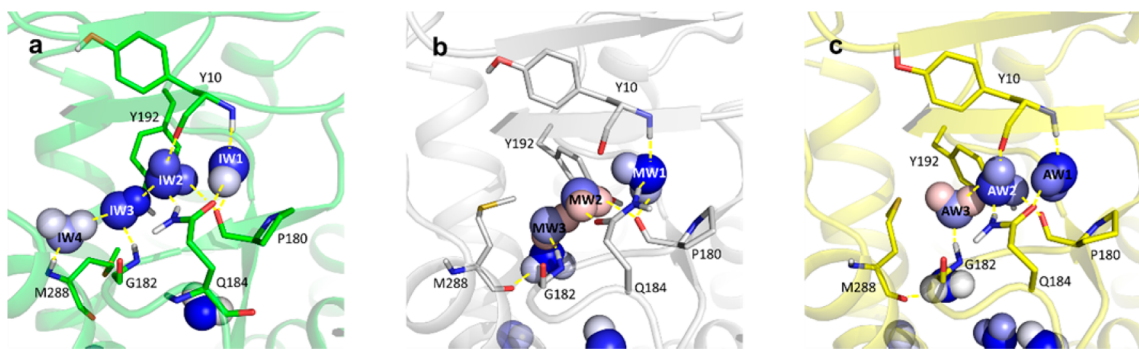


Figure 2. Functional hydration sites and the corresponding hydrogen-bond network around the extracellular region. The hydrogen bonds are represented by dashed yellow lines. (a) Four functional hydration sites, IW1, IW2, IW3, and IW4, were identified in the inactive state. These hydration sites form a hydrogen-bond network with Tyr10, Pro180, Gly182, Gln184, Tyr192, and Met288. (b) Three functional hydration sites, MW1, MW2, and MW3 were identified in the Meta II state, which form a hydrogen-bond network with Tyr10, Pro180, Gly182, Gln184, and Tyr192. (c) Three functional hydration sites, AW1, AW2, and AW3, are identified in the constitutively active state showing that the hydrogen-bond network formed in the Meta II state has been conserved.

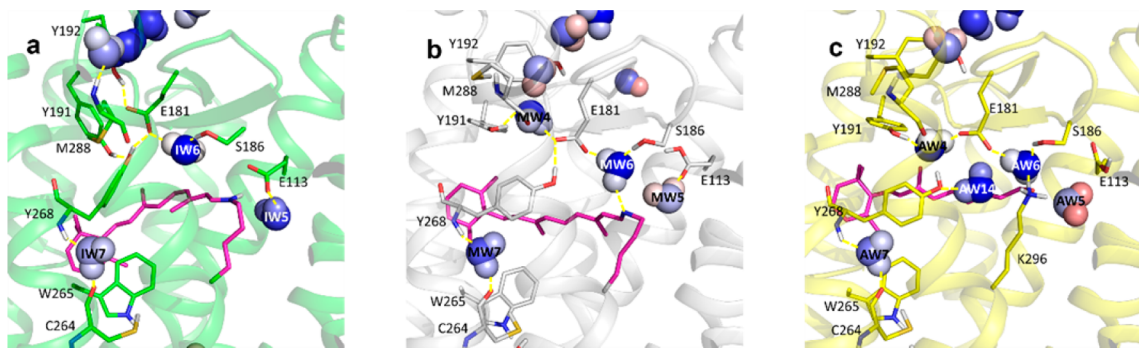


Figure 3. Functional hydration sites and the corresponding hydrogen-bond networks around the retinal. (a) Three functional hydration sites, IW5, IW6, and IW7, are identified in the inactive state. IW5 forms a hydrogen bond with Glu113 and is involved in the polar interactions with the protonated Schiff base. IW6 and IW7, together with Glu181, Ser186, Tyr191, Tyr192, Tyr268, and Cys264, form a hydrogen-bond network. (b) Four functional hydration sites, MW4, MW5, MW6, and MW7, are identified in the Meta II state. These hydration sites form a hydrogen-bond network with Glu113, the Schiff base, Ser186, Glu181, Met288, Tyr191, Tyr268, and Cys264. (c) Five functional hydration sites, AW4, AW5, AW6, AW7, and AW14, are identified in the constitutively active state. The hydrogen-bond network formed in the Meta II state is largely conserved.

In the following, we analyze the hydration sites and their functions. The distribution of these hydration sites is shown in Figure 1.

Water around the Extracellular Region. In rhodopsin, the N terminus, together with the extracellular loops (ECL1, ECL2, and ECL3), and several residues in the ligand channel play a role in retinal uptake and release.^{46–48} In particular, ECL2 has been reported to play an important role in ligand binding and receptor activation.^{47,49} Hydration sites with favorable solvation free energies have been found to connect the two hairpin structures formed by the N terminus and ECL2 and knit the hydrogen-bond networks in all the three states. In the inactive state, we identify four hydration sites (IW1, IW2, IW3, and IW4) in this region (Figure 2a). IW1 forms hydrogen bonds with Pro180 (ECL2) and the amine of Tyr10 on the N-terminal. IW2 strengthens the interaction between Tyr10 and Pro180 by forming hydrogen bonds with their backbone oxygen atoms. IW1 and IW2 also form hydrogen bonds with the side chain of Gln184 (ECL2), which further stabilizes the water molecules between the two hairpins. The hydrogen-bond network is then extended to IW3 that forms hydrogen bonds with IW2, the amine of Gly182 (ECL2), and the side chain oxygen of Tyr192 (ECL2). IW4 further extends the interactions to H7 by forming hydrogen bonds with IW3 and the amine group of Met288 (H7).

In both Meta II and constitutively active states, we identify three hydration sites that form similar interactions and hydrogen-bond networks (Figure 2b,c). An analysis of the thermodynamic signatures and positioning of the hydration sites leads us to suggest that MW1, MW2, and MW3 in the Meta II state are evolved from IW1, IW2, and IW3 in the inactive state, which are further resolved as AW1, AW2, and AW3 in the active state, respectively. Here we exemplify the characteristics of the hydrogen-bond network in the Meta II state (Figure 2b). In this state, the hydration site MW1 is located in almost the same place as IW1 in the inactive state and the hydrogen-bond network with IW1 also remains the same. The motion of ECL2 upon receptor activation triggers Tyr192 to flip and form a hydrogen bond with MW2. MW3 becomes less stable than IW3 (as indicated by the thermodynamic signatures) because of a lack of the hydrogen-bond interaction with Tyr192. The hydrogen-bond network knitted by the water molecules in this region can stabilize ECL2 in the inactive state, and, upon receptor activation, it can provide the appropriate plasticity required for ECL2 to function.

Water around the Retinal. We identify three functional hydration sites, IW5, IW6, and IW7, around the retinal in the inactive state (Figure 3a). IW5 is hydrogen-bonded to the carboxyl group of Glu113 (H3) and is involved in the polar

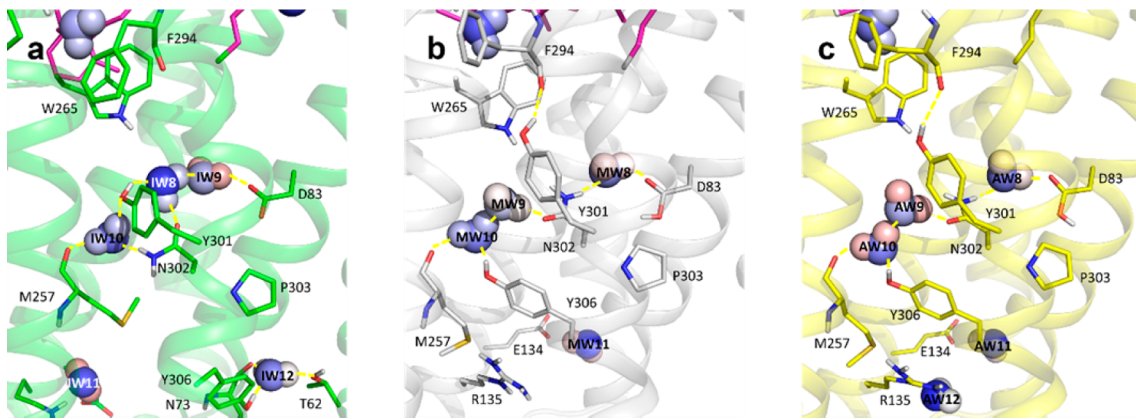


Figure 4. Functional hydration sites and the corresponding hydrogen-bond networks adjacent to the “NP_xxY” motif. (a) Four hydration sites, IW8, IW9, IW10, and IW12, are identified in the inactive state. IW8, IW9, and IW10 form a hydrogen-bond network with Asp83, Tyr301, Asn302, and Met257. IW8 also forms a polar interaction with Trp265. IW12 is hydrogen-bonded to Tyr306, Thr62, and Asn73. (b) Three hydration sites MW8, MW9, and MW10, are identified in the Meta II state. MW8, MW9, and MW10, together with Asp83, Asn302, Tyr306, and Met257, form a hydrogen-bond network. Tyr301 is excluded from the water-mediated hydrogen-bond network, but forms a hydrogen bond with Phe294. (c) Three functional hydration sites, AW1, AW2, and AW3, are identified in the constitutively active state. These hydration sites are located in similar positions and form a rather similar hydrogen-bond network as in the Meta II state.

interactions with the protonated Schiff base with a distance of 3.0 Å. The protonated Schiff base forms an electrostatic interaction with Glu113, which has been proved to play a crucial role in maintaining the receptor in the inactive conformation.^{50,51} Most likely, there exists a polar interaction between the protonated Schiff base and the nearby hydration site IW6 with a distance of 4.6 Å. Clearly, IW6 forms a hydrogen-bond network with Glu181 and Ser186 on ECL2, which further extends to Tyr192 (ECL2) and Tyr268 (H6). Tyr191 (ECL2) also contributes to this hydrogen-bond network by interacting with Tyr268. The hydration site IW7 further extends the network to Cys264 through hydrogen-bonding to the backbones of Tyr268 and Cys264 on H6.

In the activation process, one proton transfers from the protonated Schiff base to Glu113 (H3) and a conformational change around the retinal has been observed experimentally.⁵² Rearrangements of hydration sites and the hydrogen-bond network are also reflected, as indicated in the Meta II state (Figure 3b). Along with the proton transfer, the electrostatic interaction between the Schiff base and Glu113 decreases dramatically, leading to an increase of distance between them from 3.5 to 5.3 Å, and, in a location similar to that of IWS, MWS is resolved, which works as a bridge between them through the hydrogen-bond interaction. Although MWS is found to be less stable than IWS as indicated by the thermodynamic signatures, it is likely that this water molecule is involved in the hydrolysis of the covalent bond between the retinal and Lys296 as suggested by the experiments.^{24,53} A recent computational study on ultraviolet cone pigments suggested that IWS or MWS is involved in the switch of the protonated state of the Schiff base.⁵⁴ With the protonation of Glu113, IW6, together with Glu181, and the Schiff base moves closer, reducing the distance between the carboxyl group of Glu181 and the Schiff base nitrogen from 7.1 to 5.0 Å. IW6 is resolved as MW6 in this state, and the interaction between MW6 and the Schiff base becomes stronger because of the formation of a hydrogen bond between them. MW6 has not been resolved in the crystal structure, but thanks to the resolution of MW6, the rearrangement of the hydrogen-bond network can thus be identified. Accompanying with Glu181 moving toward the Schiff base, the side chain of Tyr268, which is hydrogen-bonded

to Glu181 in the inactive state, flips and the hydrogen-bond interaction between Tyr268 (H6) and Tyr191 (ECL2) is replaced by the edge to face π–π stacking interaction. Notably, a new hydration site MW4, which has not been observed experimentally, is found to be hydrogen-bonded to Tyr191, Glu181, and in particular, the backbone of Met288. MW7, which is believed to be equivalent to IW7 and hydrogen-bonded to the backbones of Tyr268 and Cys264 on H6, is suggested to define both the inactive conformation and the active conformation for the activation signal transmission to the “NP_xxY” motif.

The hydrogen-bond network formed in the activation process is largely conserved in the activated state, as reflected in the constitutively active state (Figure 3c). In this structure, the retinal is unbound to Lys296 (H7) and a structural rearrangement around it occurs. The water-bridge between Glu113 and the retinal disappears, and the carboxyl group of Glu113 flips away. The hydration sites AW6 and AW14 stabilize Lys296 by hydrogen-bonding to Glu181 and Tyr268, respectively (Figure 3c) and, together with the other two hydration sites AW5 and AW7, enhance the polarity of the retinal binding pocket. Therefore, the identification of the hydration sites around the retinal helps us understand the origin of the polar environment around the Schiff base revealed by magic angle spinning NMR spectroscopy.⁵⁵

Water Adjacent to the “NP_xxY” Motif. The “NP_xxY” motif is a key motif in the activation of family A GPCRs.^{50,51,56} In the inactive state, we identified four hydration sites, IW8, IW9, IW10, and IW12, adjacent to the motif (Figure 4a). IW8 is hydrogen-bonded to Tyr301 (H7) and Asn302 (H7), and forms a polar interaction with Trp265 (H6). IW8 also interacts with IW9, through which the hydrogen-bond network is extended to Asp83 (H2). IW10 is found to form hydrogen bonds with Tyr301 (H7), Asn302 (H7), and the backbone of Met257 (H6). Thus, IW8, IW9 and IW10, together with Asp83, Tyr301, Asn302, and Met257, form a hydrogen-bond network as proposed by Pardo et al.¹² Of interest is the identification of the hydration site IW12 in the vicinity of Tyr306 (H7), Thr62 (H1), and Asn73 (H2). The existence of water molecules has been suggested by Palczewski in order to justify the interaction between Tyr306 and Asn73.²⁸ A water molecule has been

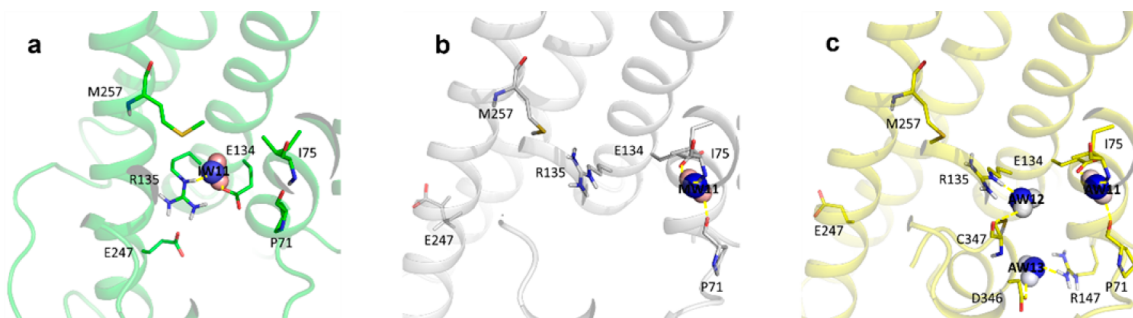


Figure 5. Functional hydration sites adjacent to the “ERY” motif in the inactive state (a), Meta II state (b), and constitutively active state (c).

observed to be hydrogen-bonded to Thr62 and to the backbone of Asn73 in the analysis of another inactive structure 1L9H.¹⁰ Our analysis demonstrates that IW12 forms hydrogen bonds with the side chains of Tyr306, Thr62 and the backbone of Asn73 and thus mediates the interactions between helices H7, H1, and H2.

The distribution of the hydration sites in the Meta II state (Figure 4b) and the constitutively active state (Figure 4c) are found to be rather similar in the “NP_{xx}Y” motif, although the hydration sites MW8 and MW10 were not observed in the former crystallography structure. Therefore, we only analyze the hydration sites and the hydrogen-bond network in the Meta II state. In this state, we identify that three hydration sites, MW8, MW9, and MW10, are associated with favorable solvation energies. These hydration sites form a hydrogen-bond network that evolves from the corresponding network in the inactive state. The side chain of Asn302 flips and forms two hydrogen bonds with MW8 and MW9. Asn302 (H7) and Asp83 (H2) are connected through the hydration site MW8, instead of through the two hydration sites IW8 and IW9 as in the inactive state. Two hydration sites, MW9 and MW10 are found to bridge Asn302 (H7) and Met257 (H6). Tyr306 flips and forms a hydrogen bond with MW10. Thus, after the activation, the local hydrogen-bond network around IW12 in the inactive state is destroyed, and the hydrogen-bond network in the motif is rearranged, which consists of Asp83, Asn302, Met257, and Tyr306, and is mediated by MW8, MW9, and MW10. Compared with the corresponding hydrogen-bond network in the inactive state, Trp265 and Tyr301 are excluded from this network, and Tyr306 is included.

Aside from the water mediated hydrogen-bond network, our methods provide the advantages to analyze the thermodynamics change of the functional water molecules in this region. Through comparing the thermodynamic signatures of the hydration sites adjacent to the “NP_{xx}Y” motif (Table S2), we observe that with the receptor evolving from the inactive state to the Meta II state, the hydration sites become less stable, as indicated by a change of the averaged solvation energy of the hydration sites from -7.05 kcal/mol to -4.95 kcal/mol, which is mainly caused by the change in the enthalpy. This reflects that the water-mediated hydrogen-bond network adjacent to the “NP_{xx}Y” motif is not as stable in the Meta II state as in the inactive states.

Water Adjacent to the “ERY” Motif. The “ERY” motif is another key functional motif in GPCR activation. Breaking of the ionic lock between Arg135 in the “ERY” motif and Glu247 in H6 has been believed to be a crucial step for GPCR activation.^{50,51} In the inactive state, we identify that there is a hydration site (IW11) located adjacent to the “ERY” motif which forms hydrogen bonds with both Arg135 and Glu134

and is likely to affect the ionic lock (Figure 5a). IW11 in the inactive state may follow the motion of Glu134 upon breaking the ionic lock during the rhodopsin activation. IW11 is resolved as MW11 in the Meta II state (Figure 5b) where the hydration site is hydrogen-bonded to the backbone of Ile75 and Pro71 on H2 and forms a local hydrogen-bond network. The hydration site MW11 thus stabilizes the local network to keep the structure in the active state.

By comparing the interfacial hydration sites in the Meta II and constitutively active states, we further identified the water molecules potentially contributing to the Gt binding in the constitutively active state where the C-terminal tail of the α -subunit of the Gt (the $\text{G}\alpha\text{CT}$ -peptide) is bound to the rhodopsin. Two hydration sites, AW12 and AW13, with favorable solvation energies are resolved at the rhodopsin- $\text{G}\alpha\text{CT}$ -peptide interface. Through hydrogen-bond interactions, AW12 connects Arg135 (H3) and Cys347 on the $\text{G}\alpha\text{CT}$ -peptide, while AW13 links Arg147 (ICL2) and Asp346 on the $\text{G}\alpha\text{CT}$ -peptide.

DISCUSSION

After determining the positioning of functional hydration sites and identifying the water-mediated hydrogen-bond networks in the inactive, Meta II, and constitutively active states, we discuss here their roles in the rhodopsin activation process in the two key regions—the region adjacent to the retinal and the “NP_{xx}Y” motif—with the aim to reveal the role of the water molecules in the activation of rhodopsin.

The role of the functional hydration site in the region adjacent to the retinal is associated with the proton transfer from the Schiff base to Glu113, which makes the hydration site IW5 in the inactive state become less stable, as in the Meta II state, and which makes it disappear in the constitutively active state. We thus suggest that this hydration site mediates the proton transfer from the Schiff base to the carboxyl group of Glu113, which is consistent with the water-mediated proton transfer mechanism proposed by the time-resolved Fourier transform infrared spectroscopy studies on bacteriorhodopsin in ref 24. IW6 is rather stable in the activation process and is resolved as the hydration sites MW6 and AW6 in the Meta II and constitutively active states, respectively. It is notable that none of the latter two sites have been observed in the respective crystallography structures. The identification of these hydration sites allows us to suggest that IW6 functions as a switch for signal transmission through regulating the distance between Glu181 and the Schiff base, which is important for understanding the activation mechanism around the Schiff base. In the inactive state, the interaction between the Schiff base and Glu181 is switched off, while when the receptor is triggered to

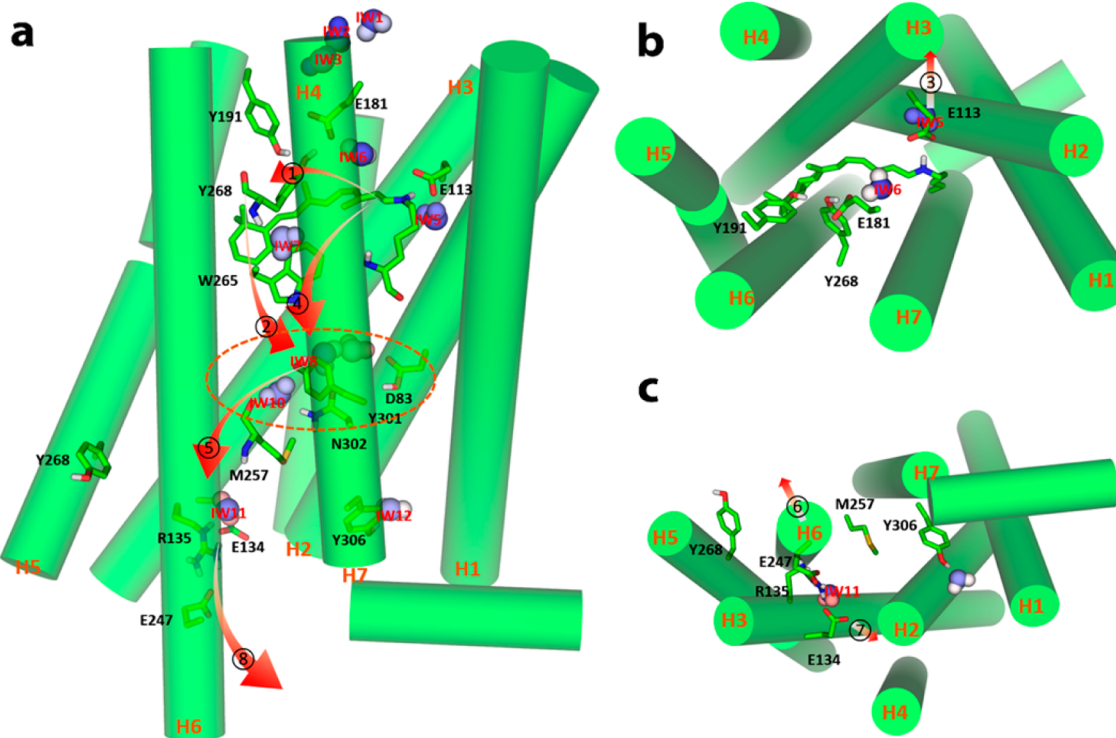


Figure 6. Hypothesis for the water-mediated rhodopsin activation pathway. (a–c) represent the front view, top view, and bottom view of the receptor, respectively. The signal transmission pathway and conformation changes upon rhodopsin activation are illustrated with red arrows.

the Meta II state or the active state, this interaction is switched on. MW4 also plays a key role in the rhodopsin activation, though this hydration site has not been observed experimentally. Through MW4, the hydrogen-bond network is extended to the backbone of Met288 (H7). In this way, the hydrogen-bond network stabilizes the active state. Mutation of Tyr191 or Tyr268 destroys the local hydrogen-bond network connecting to H7 and most likely destabilizes the active structure. We can thus explain the experimental observation pertaining to the mutation of Tyr191 and Tyr268, which results in an inefficient Meta II formation and in the formed Meta II state decaying faster than in the wild-type rhodopsin.^{57–59}

When clarifying the role of the functional hydration sites in the “NP_xxY” motif, we note that Trp265 is known to be released from the locked position in the inactive state.^{12,13} The delocalization of Trp265, together with the tilt motion of H6, destabilizes not only the hydration site IW8 but also the water-mediated hydrogen-bond network adjacent to the “NP_xxY” motif. Facilitated by the proton transfer from the protonated Schiff base to Glu113, which relaxes the helices H7 and H3, as evidenced by the $\text{C}\alpha$ distance between Lys296 (H7) and Glu113 (H3) increasing from 10.9 Å in the inactive structure to 13.5 Å in the Meta II structure (being 13.7 Å in the constitutively active structure), the hydrogen-bond network mediated by the hydration sites IW8, IW9, and IW10 rearranges. We can thus explain the breaking of the hydrogen bonds between Trp265 and Asn302 as observed by NMR.⁶⁰ Accompanied with the rearrangement of the hydrogen-bond network, Tyr301 leaves the network and forms a hydrogen bond with the backbone of Phe294 (H7). Because of the formation of this hydrogen bond, H7 is significantly compressed, as reflected by the $\text{C}\alpha$ distance between Phe294 and Tyr301, which changes from 11.6 Å in the inactive state to 10.1

Å in the Meta II and constitutively active state structures. Clearly, the formation of this hydrogen bond assists the signal propagation along the helix H7 and stabilizes the receptor in the active conformation.

Experimental investigations have provided explanations for the conformational change of rhodopsin during the activation. Based on the experimental results and functional water molecules we identified, we proposed a hypothesis for the water-mediated rhodopsin activation pathway (Figure 6). Upon photoabsorption, isomerization of the retinal is triggered. Crystal structures have confirmed that the roll of the hinge point C9-Me group on the retinal leaves space for Tyr268 to flip and the activation signal is subsequently transmitted to Tyr268 (arrow 1 in Figure 6a).^{52,61} Along with the isomerization of the retinal, one proton transfers from the protonated Schiff base to Glu113 as proposed by the prior studies.²⁵ It is interesting to see that the water-mediated hydrogen-bond network formed by the Schiff base, Ser186, Glu181, Try191, and Met288, further assists the flip motion of Tyr268 and stabilizes the activated structure, and in particular, Tyr268 in the flipped state. This results in a steric clash between Tyr268 and Trp265, leading to a subsequent motion of Trp265, which has been indicated by the crystal structures of the Meta II and constitutively active states (arrow 2 in Figure 6a).⁶² The activation signal is thus transmitted to Trp265. Interestingly, we find that the motion of Trp265 weakens the interaction between Trp265 and the water molecule IW8. Assisted by the relaxation of H7 and H3 originating from the proton transfer from the protonated Schiff base to Glu113 (arrow 3 in Figure 6b and arrow 4 in Figure 6a), the hydrogen-bond network mediated by the hydration sites IW8, IW9, and IW10 rearranges, and the water cluster around the “NP_xxY” motif becomes less stable as indicated by its thermodynamic

signatures (in the dashed red circle in Figure 6a). This in turn leads Tyr301 to form a hydrogen-bond with the backbone of Phe294 and the helix between Tyr301 and Phe294 on H7 becomes significantly compressed, bringing out a consequent motion of the remaining helix as indicated by the structure of the Meta II state. As a result, the activation signal is transmitted to Asn302. With the rearrangement of the hydrogen-bond network near Asn302, the signal is further transmitted to Met257 (arrow 5 in Figure 6a). The rearrangement of the hydrogen-bond network also weakens the hydrogen-bond interactions between H6, H3, H5 and H7 and produces an outward tilt motion of H6 (arrow 6 in c). Finally, the outward tilt motion of H6, originating from the rearrangement of the hydrogen-bond network, disrupts the ionic lock between Arg135 and Glu247 (arrow 7 in Figure 6c), and the activation signal is transmitted to the cytoplasmic G-protein binding surface (arrow 8 in Figure 6a).

CONCLUSION

The use of all-atom molecular dynamics simulations in combination with inhomogeneous fluid theory has allowed us to determine the distribution of hydration sites in rhodopsin. By applying this methodology to the inactive, Meta II, and constitutively active states, we identified the functional hydration sites essential for the rhodopsin activation. We found that in each of the key states most of the functional hydration sites are located in the regions occupied by the cocrystallized water molecules. We verified the experimental observation of water releasing during the transition from the inactive state to the Meta II state and determined the regions where the water molecules were released. We furthermore identified the hydrogen-bond networks in each state, in which some of the hydrogen bonds have hitherto not been reported. By analyzing the evolution of the functional hydration sites and the corresponding hydrogen-bond networks around key residues in different states, we suggest that one hydration site (IW6 or MW6) functions as a switch for signaling by regulating the distance between Glu181 and the Schiff base. We find that the less stable water molecules adjacent to the “NPxxY” motif in the Meta II state are closely related to the significant rearrangement of the water-mediated hydrogen-bond network in the motif, which has been believed to be essential for mediating the activation of the receptor. We can thereby suggest the function of water molecules in the rhodopsin activation. We expect this methodology to serve as an important complement to experiment in elucidating the function of water molecules in other protein receptors as well.

ASSOCIATED CONTENT

Supporting Information

Supporting Figures 1–6, supporting Tables 1 and 2, and thermodynamics signatures for all the hydration sites (data set S1). This material is available free of charge via the Internet at <http://pubs.acs.org>.

AUTHOR INFORMATION

Corresponding Author

*E-mail: tu@theochem.kth.se. Tel: + 46 (0)8 5537 8417. Fax: +46 (0)8 5537 8590. Mailing address: Division of Theoretical Chemistry and Biology School of Biotechnology, KTH Royal Institute of Technology, S-106 91 Stockholm, Sweden.

Notes

The authors declare no competing financial interest.

ACKNOWLEDGMENTS

This work was supported by a grant from the Swedish National Infrastructure for Computing (SNIC), SNIC 025/12-38. X.S. acknowledges the China Scholarship Council for financial support.

REFERENCES

- Rosenbaum, D. M.; Rasmussen, S. G. F.; Kobilka, B. K. The structure and function of G-protein-coupled receptors. *Nature* **2009**, *459*, 356–363.
- Venkatakrishnan, A. J.; Deupi, X.; Lebon, G.; Tate, C. G.; Schertler, G. F.; Babu, M. M. Molecular signatures of G-protein-coupled receptors. *Nature* **2013**, *494*, 185–194.
- Ahuja, S.; Smith, S. O. Multiple switches in G protein-coupled receptor activation. *Trends Pharmacol. Sci.* **2009**, *30*, 494–502.
- Kobilka, B. K. G protein coupled receptor structure and activation. *Biochim. Biophys. Acta, Biomembr.* **2007**, *1768*, 794–807.
- Tesmer, J. J. G. The quest to understand heterotrimeric G protein signaling. *Nat. Struct. Mol. Biol.* **2010**, *17*, 650–652.
- Jardón-Valadez, E.; Bondar, A.-N.; Tobias, D. J. Coupling of retinal, protein, and water dynamics in squid rhodopsin. *Biophys. J.* **2010**, *99*, 2200–2207.
- Jardón-Valadez, E.; Bondar, A.-N.; Tobias, D. J. Dynamics of the internal water molecules in squid rhodopsin. *Biophys. J.* **2009**, *96*, 2572–2576.
- Angel, T. E.; Chance, M. R.; Palczewski, K. Conserved waters mediate structural and functional activation of family A (rhodopsin-like) G protein-coupled receptors. *Proc. Natl. Acad. Sci. U. S. A.* **2009**, *106*, 8555–8560.
- Angel, T. E.; Gupta, S.; Jastrzebska, B.; Palczewski, K.; Chance, M. R. Structural waters define a functional channel mediating activation of the GPCR, rhodopsin. *Proc. Natl. Acad. Sci. U. S. A.* **2009**, *106*, 14367–14372.
- Okada, T.; Fujiyoshi, Y.; Silow, M.; Navarro, J.; Landau, E. M.; Shichida, Y. Functional role of internal water molecules in rhodopsin revealed by X-ray crystallography. *Proc. Natl. Acad. Sci. U. S. A.* **2002**, *99*, 5982–5987.
- Liu, J.; Liu, M. Y.; Nguyen, J. B.; Bhagat, A.; Mooney, V.; Yan, E. C. Y. Thermal properties of rhodopsin: Insight into the molecular mechanism of dim-light vision. *J. Biol. Chem.* **2011**, *286*, 27622–27629.
- Pardo, L.; Deupi, X.; Dölker, N.; López-Rodríguez, M. L.; Campillo, M. The role of internal water molecules in the structure and function of the rhodopsin family of G protein-coupled receptors. *ChemBioChem* **2007**, *8*, 19–24.
- Standfuss, J.; Edwards, P. C.; D’Antona, A.; Fransen, M.; Xie, G.; Oprian, D. D.; Schertler, G. F. The structural basis of agonist-induced activation in constitutively active rhodopsin. *Nature* **2011**, *471*, 656–660.
- Carugo, O. Correlation between occupancy and B factor of water molecules in protein crystal structures. *Protein Eng.* **1999**, *12*, 1021–1024.
- Lazaridis, T. Inhomogeneous fluid approach to solvation thermodynamics. 1. Theory. *J. Phys. Chem. B* **1998**, *102*, 3531–3541.
- Wang, L.; Berne, B. J.; Friesner, R. A. Ligand binding to protein-binding pockets with wet and dry regions. *Proc. Natl. Acad. Sci. U. S. A.* **2011**, *108*, 1326–1330.
- Abel, R.; Young, T.; Farid, R.; Berne, B. J.; Friesner, R. A. Role of the active-site solvent in the thermodynamics of factor Xa ligand binding. *J. Am. Chem. Soc.* **2008**, *130*, 2817–31.
- Li, Z.; Lazaridis, T. Thermodynamics of buried water clusters at a protein–ligand binding interface. *J. Phys. Chem. B* **2006**, *110*, 1464–1475.
- Li, Z.; Lazaridis, T. Water at biomolecular binding interfaces. *Phys. Chem. Chem. Phys.* **2007**, *9*, 573.

- (20) Li, Z.; Lazaridis, T. Thermodynamic contributions of the ordered water molecule in HIV-1 protease. *J. Am. Chem. Soc.* **2003**, *125*, 6636–6637.
- (21) Young, T.; Abel, R.; Kim, B.; Berne, B. J.; Friesner, R. A. Motifs for molecular recognition exploiting hydrophobic enclosure in protein–ligand binding. *Proc. Natl. Acad. Sci. U.S.A.* **2007**, *104*, 808–813.
- (22) Higgs, C.; Beuming, T.; Sherman, W. Hydration site thermodynamics explain SARs for triazolylpurines analogues binding to the A2A receptor. *ACS Med. Chem. Lett.* **2010**, *1*, 160–164.
- (23) Khavrutskii, I. V.; Wallqvist, A. Improved binding free energy predictions from single-reference thermodynamic integration augmented with hamiltonian replica exchange. *J. Chem. Theory. Comput.* **2011**, *7*, 3001–3011.
- (24) Garczarek, F.; Gerwert, K. Functional waters in intraprotein proton transfer monitored by FTIR difference spectroscopy. *Nature* **2006**, *439*, 109–112.
- (25) Hofmann, K. P.; Scheerer, P.; Hildebrand, P. W.; Choe, H.-W.; Park, J. H.; Heck, M.; Ernst, O. P. A G protein-coupled receptor at work: The rhodopsin model. *Trends Biochem. Sci.* **2009**, *34*, 540–552.
- (26) Smith, S. O. Structure and activation of the visual pigment rhodopsin. *Annu. Rev. Biophys.* **2010**, *39*, 309–328.
- (27) Hayashi, S.; Tajkhorshid, E.; Kandori, H.; Schulten, K. Role of hydrogen-bond network in energy storage of bacteriorhodopsin's light-driven proton pump revealed by ab initio normal-mode analysis. *J. Am. Chem. Soc.* **2004**, *126*, 10516–10517.
- (28) Palczewski, K. G protein-coupled receptor rhodopsin. *Annu. Rev. Biochem.* **2006**, *75*, 743–67.
- (29) Choe, H.-W.; Kim, Y. J.; Park, J. H.; Morizumi, T.; Pai, E. F.; Krausz, N.; Hofmann, K. P.; Scheerer, P.; Ernst, O. P. Crystal structure of metarhodopsin II. *Nature* **2011**, *471*, 651–655.
- (30) Okada, T.; Sugihara, M.; Bondar, A.-N.; Elstner, M.; Entel, P.; Buss, V. The retinal conformation and its environment in rhodopsin in light of a new 2.20 Å crystal structure. *J. Mol. Biol.* **2004**, *342*, 571–583.
- (31) Berman, H. M.; Westbrook, J.; Feng, Z.; Gilliland, G.; Bhat, T. N.; Weissig, H.; Shindyalov, I. N.; Bourne, P. E. The protein data bank. *Nucleic Acids Res.* **2000**, *28*, 235–42.
- (32) Fahmy, K.; Jäger, F.; Beck, M.; Zvyaga, T. A.; Sakmar, T. P.; Siebert, F. Protonation states of membrane-embedded carboxylic acid groups in rhodopsin and metarhodopsin II: A Fourier-transform infrared spectroscopy study of site-directed mutants. *Proc. Natl. Acad. Sci. U. S. A.* **1993**, *90*, 10206–10210.
- (33) Lüdeke, S.; Beck, M.; Yan, E. C. Y.; Sakmar, T. P.; Siebert, F.; Vogel, R. The role of Glu181 in the photoactivation of rhodopsin. *J. Mol. Biol.* **2005**, *353*, 345–356.
- (34) Nagata, T.; Terakita, A.; Kandori, H.; Shichida, Y.; Maeda, A. The hydrogen-bonding network of water molecules and the peptide backbone in the region connecting Asp83, Gly120, and Glu113 in bovine rhodopsin. *Biochemistry* **1998**, *37*, 17216–17222.
- (35) Yan, E. C. Y.; Kazmi, M. A.; Ganim, Z.; Hou, J.-M.; Pan, D.; Chang, B. S. W.; Sakmar, T. P.; Mathies, R. A. Retinal counterion switch in the photoactivation of the G protein-coupled receptor rhodopsin. *Proc. Natl. Acad. Sci. U. S. A.* **2003**, *100*, 9262–9267.
- (36) Frähmcke, J. S.; Wanko, M.; Phatak, P.; Mroginski, M. A.; Elstner, M. The protonation state of Glu181 in rhodopsin revisited: Interpretation of experimental data on the basis of QM/MM calculations. *J. Phys. Chem. B* **2010**, *114*, 11338–11352.
- (37) Schrödinger Suite 2013 Protein Preparation Wizard, Epik version 2.5; Schrödinger, LLC: New York, 2013.
- (38) Humphrey, W.; Dalke, A.; Schulten, K. VMD: visual molecular dynamics. *J. Mol. Graph.* **1996**, *14*, 33–8.
- (39) Phillips, J. C.; Braun, R.; Wang, W.; Gumbart, J.; Tajkhorshid, E.; Villa, E.; Chipot, C.; Skeel, R. D.; Kalé, L.; Schulten, K. Scalable molecular dynamics with NAMD. *J. Comput. Chem.* **2005**, *26*, 1781–1802.
- (40) Vanommeslaeghe, K.; Hatcher, E.; Acharya, C.; Kundu, S.; Zhong, S.; Shim, J.; Darian, E.; Guvench, O.; Lopes, P.; Vorobyov, I.; et al. CHARMM general force field: A force field for drug-like molecules compatible with the CHARMM all-atom additive biological force fields. *J. Comput. Chem.* **2010**, *31*, 671–690.
- (41) Frisch, M. J.; Trucks, G. W.; Schlegel, H. B.; Scuseria, G. E.; Robb, M. A.; Cheeseman, J. R.; Scalmani, G.; Barone, V.; Mennucci, B.; Petersson, G. A.; et al. Gaussian 09, revision A.02; Gaussian, Inc.: Wallingford CT, 2009.
- (42) Lazaridis, T.; Karplus, M. Orientational correlations and entropy in liquid water. *J. Chem. Phys.* **1996**, *105*, 4294–4316.
- (43) Mitchell, D. C.; Litman, B. J. Effect of protein hydration on receptor conformation: decreased levels of bound water promote metarhodopsin II formation. *Biochemistry* **1999**, *38*, 7617–7623.
- (44) Ruprecht, J. J.; Mielke, T.; Vogel, R.; Villa, C.; Schertler, G. F. X. Electron crystallography reveals the structure of metarhodopsin I. *EMBO J.* **2004**, *23*, 3609–3620.
- (45) Wald, G.; Durell, J.; St. George, R. C. C. The light reaction in the bleaching of rhodopsin. *Science* **1950**, *111*, 179–181.
- (46) Bourne, H. R.; Meng, E. C. Rhodopsin sees the light. *Science* **2000**, *289*, 733–734.
- (47) Ahuja, S.; Hornak, V.; Yan, E. C. Y.; Syrett, N.; Goncalves, J. A.; Hirshfeld, A.; Ziliox, M.; Sakmar, T. P.; Sheves, M.; Reeves, P. J.; et al. Helix movement is coupled to displacement of the second extracellular loop in rhodopsin activation. *Nat. Struct. Mol. Biol.* **2009**, *16*, 168–175.
- (48) Piechnick, R.; Ritter, E.; Hildebrand, P. W.; Ernst, O. P.; Scheerer, P.; Hofmann, K. P.; Heck, M. Effect of channel mutations on the uptake and release of the retinal ligand in opsin. *Proc. Natl. Acad. Sci. U. S. A.* **2012**, *109*, 5247–5252.
- (49) Wheatley, M.; Wootten, D.; Conner, M. T.; Simms, J.; Kendrick, R.; Logan, R. T.; Poyner, D. R.; Barwell, J. Lifting the lid on GPCRs: The role of extracellular loops. *Br. J. Pharmacol.* **2012**, *165*, 1688–1703.
- (50) Stenkamp, R. E.; Teller, D. C.; Palczewski, K. Rhodopsin: A structural primer for G-protein coupled receptors. *Arch. Pharm.* **2005**, *338*, 209–216.
- (51) Trzaskowski, B.; Latek, D.; Yuan, S.; Ghoshdastider, U.; Debinski, A.; Filippek, S. Action of molecular switches in GPCRs—Theoretical and experimental studies. *Curr. Med. Chem.* **2012**, *19*, 1090–109.
- (52) Knierim, B.; Hofmann, K. P.; Ernst, O. P.; Hubbell, W. L. Sequence of late molecular events in the activation of rhodopsin. *Proc. Natl. Acad. Sci. U. S. A.* **2007**, *104*, 20290–20295.
- (53) Jastrzebska, B.; Palczewski, K.; Golczak, M. Role of bulk water in hydrolysis of the rhodopsin chromophore. *J. Biol. Chem.* **2011**, *286*, 18930–18937.
- (54) Sekharan, S.; Mooney, V. L.; Rivalta, I.; Kazmi, M. A.; Neitz, M.; Neitz, J.; Sakmar, T. P.; Yan, E. C. Y.; Batista, V. S. Spectral tuning of ultraviolet cone pigments: An interhelical lock mechanism. *J. Am. Chem. Soc.* **2013**, *135*, 19064–19067.
- (55) Ahuja, S.; Eilers, M.; Hirshfeld, A.; Yan, E. C. Y.; Ziliox, M.; Sakmar, T. P.; Sheves, M.; Smith, S. O. 6-s-cis Conformation and polar binding pocket of the retinal chromophore in the photoactivated state of rhodopsin. *J. Am. Chem. Soc.* **2009**, *131*, 15160–15169.
- (56) Fritze, O.; Filippek, S.; Kuksa, V.; Palczewski, K.; Hofmann, K. P.; Ernst, O. P. Role of the conserved NPxxY(x)_{5,6}F motif in the rhodopsin ground state and during activation. *Proc. Natl. Acad. Sci. U. S. A.* **2003**, *100*, 2290–5.
- (57) Lewis, M. R.; Kono, M. Rhodopsin deactivation is affected by mutations of Tyr191. *Photochem. Photobiol.* **2006**, *82*, 1442–1446.
- (58) Doi, T.; Molday, R. S.; Khorana, H. G. Role of the intradiscal domain in rhodopsin assembly and function. *Proc. Natl. Acad. Sci. U. S. A.* **1990**, *87*, 4991–4995.
- (59) Ridge, K. D.; Bhattacharya, S.; Nakayama, T. A.; Khorana, H. G. Light-stable rhodopsin. II. An opsin mutant (TRP-265→Phe) and a retinal analog with a nonisomerizable 11-cis configuration form a photostable chromophore. *J. Biol. Chem.* **1992**, *267*, 6770–6775.
- (60) Patel, A. B.; Crocker, E.; Reeves, P. J.; Getmanova, E. V.; Eilers, M.; Khorana, H. G.; Smith, S. O. Changes in interhelical hydrogen bonding upon rhodopsin activation. *J. Mol. Biol.* **2005**, *347*, 803–812.

- (61) Mahalingam, M.; Martínez-Mayorga, K.; Brown, M. F.; Vogel, R. Two protonation switches control rhodopsin activation in membranes. *Proc. Natl. Acad. Sci. U. S. A.* **2008**, *105*, 17795–17800.
- (62) Struts, A. V.; Salgado, G. F. J.; Tanaka, K.; Krane, S.; Nakanishi, K.; Brown, M. F. Structural analysis and dynamics of retinal chromophore in dark and meta I states of rhodopsin from ^2H NMR of aligned membranes. *J. Mol. Biol.* **2007**, *372*, 50–66.